Available online at www.sciencedirect.com
ScienceDirect
Journal of Power Sources 180 (2008) 821–829
JOURNAL OF POWER SOURCES
www.elsevier.com/locate/jpowsour

Model-based power control strategy development of a fuel cell hybrid vehicle

Yun Haitao [a,b,*], Zhao Yulan [a], Sun Zechang [b], Wan Gang [b]

[a] School of Automobile and Traffic, Qingdao Technological University, Qingdao Shandong 266033, China
[b] School of Automobile, Tongji University, ShangHai 201804, China

Received 18 November 2007; received in revised form 20 January 2008; accepted 21 January 2008
Available online 2 February 2008

Abstract

An integrated procedure for math modeling and power control strategy design for a fuel cell hybrid vehicle (FCHV) is presented in this paper. Dynamic math model of the powertrain is constructed firstly, which includes four modules: fuel cell engine, DC/DC inverter, motor-driver, and power battery. Based on the mathematic model, a power control principle is designed, which uses full-states closed-loop feedback algorithm. To implement full-states feedback, a Luenberger state observer is designed to estimate open circuit voltage (OCV) of the battery, which make the control principle not sensitive to the battery SOC (state of charge) estimated error. Full-states feedback controller is then designed through analyzing step responding of the powertrain and test data. At last of the paper, the results of simulation and field test are illustrated. The results show that the power control strategy designed takes into account the performance and economy characteristics of components of the FCHV powertrain and achieves the control object excellently.

Keywords: Fuel cell hybrid vehicle; Modeling; Powertrain; Control

1. Introduction

In recent 10 years, with the problems of energy shortage and air-pollution become more and more serious, interest in alternative automotive powertrain increases steadily. As one substitute for traditional vehicle, fuel cell vehicles (FCV) have become a research hotspot in area of clean vehicle technology. The main purpose of this paper is to describe the model-based development processes of the FCV power control strategy which is applied in Tongji University START3 prototype fuel cell hybrid vehicle (FCHV).

As the automotive engine, fuel cells have some problems such as slow responding, difficulty cold starting, and braking energy cannot be recycled. So power battery is applied in FCV powertrain usually. This is so-called fuel cell hybrid vehicle. Most major vehicle manufactures have developed prototype FCV for technology evaluation and demonstration purpose [1–3]. However, since these vehicles are not meant for production, they are put together swiftly. Model-based, systematic development processes that are commonly adopted for traditional (internal combustion engine powered) vehicles, are rarely explored to their full potential in the development of these prototype vehicles.

Academic research groups are also working actively on this emerging technology. Guezennec et al. [4] solved the supervisory control problem of a FCHV as a quasi-static optimization problem and found that hybridization can significantly improve the fuel economy of FCVs. Mohsen Mohammadian et al. [5] deal a control strategy developed for optimizing the energy flow by using evolutionary algorithms implemented on a fuel cell hybrid vehicle to reach the best performance, fuel economy, emission and acceptable operation of this hybrid structure. The National Renewable Energy Laboratory included a fuel cell system option in its simulation model ADVISOR [6], which can simulate FCVs and HEVs with ease.

Up to today, few papers have published detailed models of a FCHV powertrain, and model-based, systematic development processes was not used in control design for FCHV powertrain.

* Corresponding author at: School of Automobile and Traffic, Qingdao Technological University, Street: No.2 Changjiang Middle Road, Qingdao Economic & Technological Development Area, Qingdao Shandong 266520, China. Tel.: +86 532 8687 6910; mobile: +86 13465811386.
E-mail address: yunht@163.com (Y. Haitao).

0378-7753/$ – see front matter © 2008 Elsevier B.V. All rights reserved.
doi:10.1016/j.jpowsour.2008.01.041

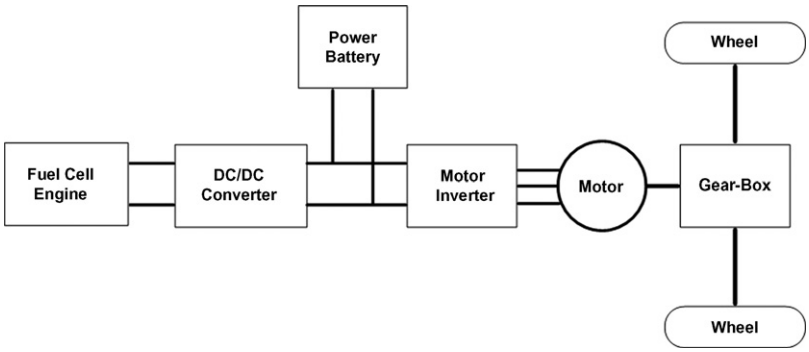

Fig. 1. Schematic configuration of the START3 FCHV.

The major feature of this study is model-based control system design for FCHV powertrain. Which is carried out by three steps: firstly, a state-space mathematic model of the FCHV powertrain is formulated based on its equivalent circuit model and test data. Then, power control strategy is developed based on the mathematic model, which uses full-states feedback algorithm. At last, the strategy is validated by simulation and field test.

2. State-space mathematic model of the powertrain

2.1. Equivalent circuit model of the powertrain

The FCHV studied in this paper is Tongji University START3 prototype vehicle. The powertrain configuration of START3 is shown in Fig. 1. A permanent magnet synchronization motor drives wheels through a slow-down gear-box. The electric motor inverter uses vector control strategy and the electric motor can work in four quadrants. A DC-DC converter (DC/DC) is placed between fuel cell engine (FCE) and the motor inverter, its purpose is to compensate the over soft output characteristic of FCE, namely resistance matching. A Li-ion battery is parallel connected to main circuit, as assistant power source, its function is recycling braking energy, providing peak power, and helping with the transient part of power load.

In the powertrain of START3, the DC/DC is current control and the motor is torque control, so both of them can be regarded as a constant current source. Bus voltage of the main circuit is equivalent to output voltage of battery. An equivalent circuit model can be abstracted consequently, as shown in Fig. 2. In this equivalent circuit model, battery is represented by a third-order equivalent circuit model which is proposed and validated in [7].

2.2. Test bench

Most components of START3 powertrain were designed specifically. They were bench-tested for factory acceptance before vehicle integration. A test bench was constructed, which enables more precise and controlled testing of individual components. In addition to subsystem function verifications, special-purpose tests were also designed to obtain the necessary data to build dynamic model and efficiency map of the subsystems.

The component configuration of test bench for fuel cell engine and electric motor is roughly same as the powertrain of START3 while an electric power load system (supplied by Arbin) was used to simulate the power load or power source. The DC/DC and battery pack were tested using the test bench which was designed specially.

2.3. Mathematic modeling

2.3.1. FCE model

In the powertrain control system, the input command of FCE is power setting P_{fset}, the output is upper limit of output power P_{Lmt}. One fact should be known is that in the powertrain system, P_{Lmt} only denote the real-time output capacity of FCE, but not the real-time output power of FCE. Real-time output power of FCE is influenced by power load and battery SOC (state of charge). According to [8], FCE is a nonlinear dynamic system, and in fuel cell control level FCE model must be nonlinear and very complicated. But in powertrain control level too complicated FCE model is unnecessary. In the powertrain control system, the relationship between P_{Lmt} and P_{fset} is just the FCE model. According to [8] and bench test data (Fig. 3), the relationship between them can be simplified as a first-order system approximately, as the transfer function shown in Eq. (1). In Fig. 3, it also can be seen that time constant of the first-order function is just little different in anterior time and posterior time.

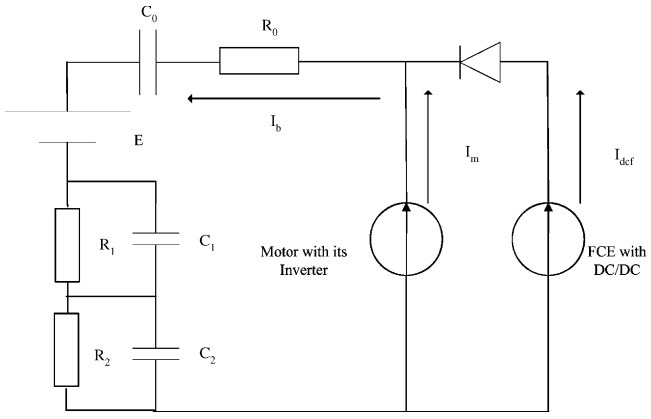

Fig. 2. Equivalent circuit model of the FCHV powertrain. Where I_{m}: current of the motor; I_{dcf}: current of the DC/DC; I_{b}: current of the battery; R_0,R_1,R_2: equivalent resistant; C_0,C_1,C_2: equivalent capacitance; E: equivalent voltage.

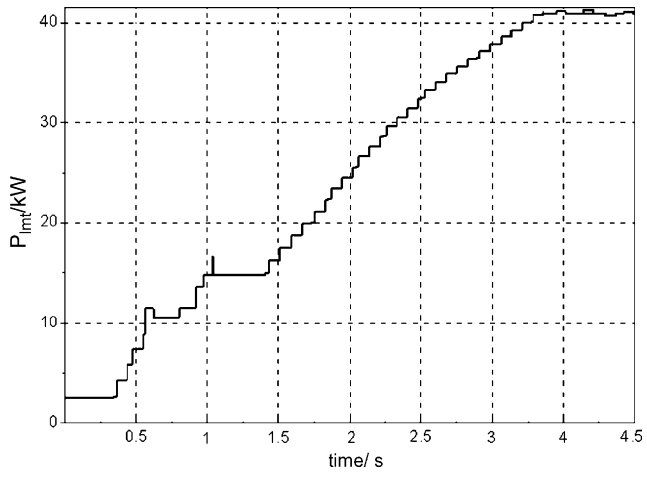

Fig. 3. Relation between P_{fset} and P_{Lmt} in bench-test (where $P_{\text{fset}} = 40$ Kw).

The simplification is advisable for mathematic modeling and control system design, and it will also be justified by model parameters estimation and validation later.

$$G_{\text{Kfce}}(\text{s}) = \frac{P_{\text{Lmt}}(\text{s})}{P_{\text{fSet}}(\text{s})} = \frac{K_{\text{fce}}}{T_{\text{fce}}\text{s} + 1} \tag{1}$$

where K_{fce}, T_{fce}: constants.

2.3.2. DC/DC model

The input command of DC/DC is current setting I_{dcfset}, the output is actual current I_{dcf}. According to the bench test data (Fig. 4), the relationship between them can be simplified as a first-order system, as the transfer function shown in (2). The simplification is advisable for mathematic modeling and control system design, and it will also be justified by model parameters estimation and validation later.

$$G_{\text{Kdcf}}(s) = \frac{I_{\text{dcf}}(s)}{I_{\text{dcfSet}}(s)} = \frac{K_{\text{dcf}}}{T_{\text{dcf}}s + 1} \tag{2}$$

where K_{dcf}, T_{dcf}: constants.

In practice, response speed of the DC/DC is slowed down to protect FCE, namely I_{dcfset} is limited by P_{Lmt}. To reflect this relationship in mathematic model, I_{dcfset} is set to upper limit and

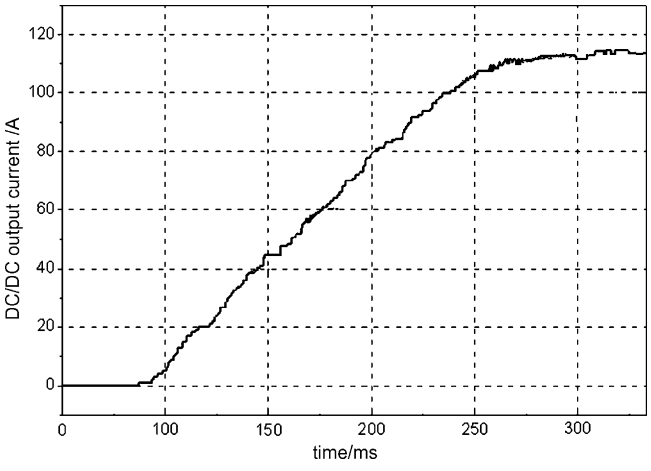

Fig. 4. Relation between I_{dcfset} and I_{dcf} in bench-test (where $I_{\text{dcfset}} = 110$ A).

the FCE and DC/DC are looked as one current source. According to Eq. (1) and (2) this current source can be denoted by transfer function, as shown in the following equation:

$$G_{\text{Kf}}(s) = \frac{I_{\text{dcf}}(s)}{I_{\text{dcfSet}}(s)} = \left(\frac{K_{\text{dcf}}}{T_{\text{dcf}}s + 1}\right)\left(\frac{K_{\text{fce}}}{T_{\text{fce}}s + 1}\right) \tag{3}$$

where U_{bus}: bus voltage. Because Figs. 3 and 4 show that responding speed of DC/DC is much fast than that of FCE (about 20:1), T_{dcf} can be omitted in simplified mathematic model. Eq. (3) can be simplified as

$$G_{\text{Kf}}(s) = \frac{I_{\text{dcf}}(s)}{I_{\text{dcfSet}}(s)} = \frac{K_{\text{dcf}}K_{\text{fce}}}{T_{\text{fce}}s + 1} = \frac{K_f}{T_f s + 1} \tag{4}$$

where $K_f = K_{\text{dcf}}K_{\text{fce}}$, $T_f = T_{\text{fce}}$.

2.3.3. Motor-driver model

The input command of electric motor inverter is torque setting Tq_{set}, the output is actual torque Tq_{Is}. Because bench-test data shows that the electric motor respond very fast, and the relationship between its output and input is linear, it can be described by a first-order system, as the transfer function shown in the following equation:

$$G_{\text{Kmc}}(s) = \frac{\text{Tq}_{\text{Is}}(s)}{\text{Tq}_{\text{Set}}(s)} = \frac{K_{\text{mc}}}{T_{\text{mc}}s + 1} \tag{5}$$

where K_{mc}, T_{mc}: constants. Because the electric motor current is function of its torque, Eq. (5) is modified as

$$G_{\text{Km}}(\text{s}) = \frac{I_{\text{m}}(\text{s})}{I_{\text{mset}}(\text{s})} = \frac{\text{Tq}_{\text{Is}}(\text{s})}{\text{Tq}_{\text{Set}}(\text{s})} = \frac{K_{\text{mc}}}{T_{\text{mc}}\text{s} + 1} \tag{6}$$

2.3.4. Battery model

As shown in Fig. 2, the battery is simulated by the third-order RC circuit model which has transfer functions shown in the following equation:

$$\begin{aligned} G_{Kb0} &= \frac{U_0(s)}{I_{\text{b}}(s)} = -\frac{1}{C_0 s} \\ G_{Kb1} &= \frac{U_1(s)}{I_{\text{b}}(s)} = -\frac{R_1}{R_1C_1s + 1} \\ G_{Kb2} &= \frac{U_2(s)}{I_{\text{b}}(s)} = -\frac{R_2}{R_2C_2s + 1} \end{aligned} \tag{7}$$

where I_{b}: battery current, U_0, U_1, U_2: voltages across C_0, C_1, C_2. According to [3], U_0 is equivalent to open circuit voltage (OCV) of the battery.

Uniting the Eq. (4), (6) and (7) and taking inverse Laplace transform, a state-pace model of the powertrain emerge as shown in the following equation:

$$\begin{cases} \dot{x} = Ax + Bu \\ y = Cx + Du \end{cases} \tag{8}$$

where state vector $\mathbf{x} = [I_{\text{dcf}}\, I_{\text{m}}\, U_0\, U_1\, U_2]^{\text{T}}$, input vector $\mathbf{u} = [P_{\text{fset}}\, I_{\text{dcfset}}\, I_{\text{mset}}]^{\text{T}}$, output vector $\mathbf{y} = [I_{\text{dcf}}\, I_m\, U_{\text{bus}}\, P_{\text{lmt}}]^{\text{T}}$. A, B, C, D

are state matrix which are defined in Eq. (9).

$$A = \begin{bmatrix} -\frac{1}{T_f} & 0 & 0 & 0 & 0 \\ 0 & -\frac{1}{T_{mc}} & 0 & 0 & 0 \\ \frac{1}{C_0} & -\frac{1}{C_0} & 0 & 0 & 0 \\ \frac{1}{C_1} & -\frac{1}{C_1} & 0 & -\frac{1}{R_1 C_1} & 0 \\ \frac{1}{C_2} & \frac{1}{C_2} & 0 & 0 & -\frac{1}{R_2 C_2} \end{bmatrix},$$

$$B = \begin{bmatrix} 0 & \frac{K_f}{T_f} & 0 \\ 0 & 0 & \frac{K_{mc}}{T_{mc}} \\ 0 & 0 & 0 \\ 0 & 0 & 0 \\ 0 & 0 & 0 \end{bmatrix} \quad (9)$$

$$C = \begin{bmatrix} R_0 & -R_0 & 1 & 1 & 1 \end{bmatrix}, D = \begin{bmatrix} 0 & 0 \end{bmatrix}$$

2.4. Model parameters estimation

There are several unknown parameters in the mathematic model developed above. To estimate these parameters, the quadratic least squares parameter estimation method is utilized in this paper. It is a method for linear regression that determines the values of unknown quantities in a statistical model by minimizing the sum of the squared residuals (expounded in [9] and [10]). Sample data came from the bench-test. To evaluate precision of the estimation, a variable called average-error-rate is defined in the following equation:

$$Ee = E(e) = \frac{1}{L}\left(\sum_{k=1}^{L}\left|\frac{z(k) - h^T(k)\widehat{\theta}_{\mathrm{LS}}}{z(k) - z_{\mathrm{base}}}\right|\right) \quad (10)$$

where L: quantity of the sample data, z_{base} is reference value of output in simulation, $h(k)$ is state vector in simulation, $\widehat{\theta}_{\mathrm{LS}}$ are estimated value of the parameters.

2.4.1. Sample data

According to reference [9], sample data is very important for parameters estimation. To make estimation result more adapted to real cycle, in bench-test input command (namely input excitation signals) are designed elaborately to simulate real cycle condition. Four kinds of cycle, including UDDS, ECE-EUDC, J1015 and FAST, are used in bench-test. Fig. 5 shows related data in UDDS cycle.

2.4.2. Parameters estimation result

In this work, the parameters are estimated based on the quadratic least squares analysis by using Matlab. The estimation results are shown in Table 1. To show the estimation precision clearly, comparison between subsystem model simulation result and test data is shown in Fig. 6.

Table 1
Model parameters estimation result

	FAST	UDDS	EC_EUDC	J1015	mean	*Ee* (%)
K_{fce}	0.9943	1.0172	0.9981	1.0227	1.008	9.19
T_{fce}	0.9957	1.0831	0.9214	1.1747	1.0437	
K_{dcf}	0.9723	0.9566	0.9566	0.9592	0.9612	3.85
T_{dcf}	0.3162	0.3386	0.303	0.3091	0.3167	
K_{mc}	0.9697	0.9852	0.9814	0.9863	0.9806	3.37
T_{mc}	0.0703	0.1015	0.0962	0.0684	0.0841	
C_0	896.94	962.87	1001.87	709.88	892.89	5.8
R_0	0.0993	0.1058	0.1067	0.0909	0.1007	
C_1	6.3006	6.4876	9.4997	5.1079	6.8490	
R_1	0.0743	0.074	0.0601	0.0385	0.0617	
C_2	115.63	127.92	95.191	154.26	123.25	
R_2	0.1771	0.1683	0.1777	0.1134	0.1591	

A FCHV powertrain simulation model is constructed based on the mathematic model in Matlab/simulink. Even though each subsystem is modeled and validated separately, the state-space model needs to be checked to confirm that the overall model works properly. The validation is done by comparing simulation result with actual test data. The motor torque demand in bench-test is given to the simulation model as the input.

To evaluate precision of the simulation, a variable is defined in Eq. (11), which is similar to the variable defined in Eq. (10).

$$Ee' = \frac{1}{L}\left(\sum_{k=1}^{L}\left|\frac{z(k) - z_{\mathrm{sim}}(k)}{z(k) - z_{\mathrm{base}}}\right|\right) \quad (11)$$

In Eq. (11), $Z_{\mathrm{sim}}(k)$ is simulation result.

The simulation precision is shown in Table 2. Fig. 7 is comparison example between simulation result and actual test data. The validation results confirm that the powertrain simulation model is reasonably accurate and the state-space mathematic model is suitable for math-based control system development.

3. Power control strategy development

Based on the state-space mathematic model shown in Eq. (9) and parameters estimation results shown in Table 1, system transfer function and pole points can be figured out, as shown below:

$$W(s) = C(sI - A)^{-1}B = \begin{bmatrix} \frac{0.126\,(s+0.8819)\,(s+0.1061)\,(s+0.005547)}{s\,(s+0.0534)\,(s+0.73)\,(s+1.25)} \\ \frac{-0.0099181\,(s+0.8819)\,(s+0.1061)\,(s+0.005547)}{s\,(s+0.0534)\,(s+0.73)\,(s+33.33)} \end{bmatrix}^T \quad (12)$$

Table 2
Model simulation precision (Eé %) in different cycle

	FAST	UDDS	EC_EUDC	J1015	mean
I_{m}	3.91	2.97	3.15	3.31	3.34
I_{dcf}	4.61	4.32	3.98	4.13	4.26
I_{b}	6.31	6.11	4.73	5.58	5.68
U_{bus}	7.74	6.63	5.12	6.13	6.41

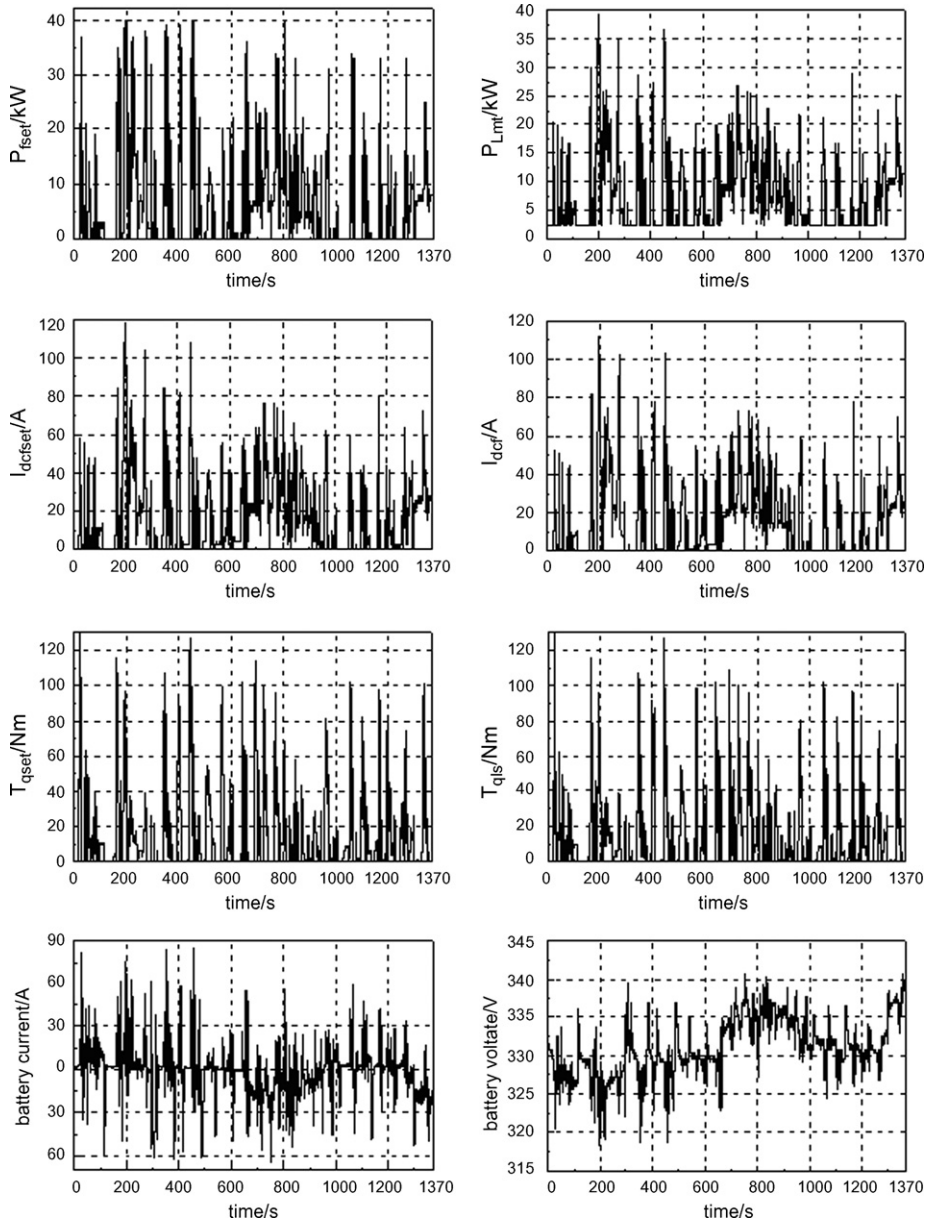

Fig. 5. Sample data for parameter estimation in UDDS cycle.

$\therefore s_1 = 0, s_2 = -0.73, s_3 = -0.0534,$

$s_4 = -1.25, s_5 = -33.33$

In Eq. (12) it can be seen that there is one pole point equals zero. According to Lyapunov's stability theory [10], it can be concluded that the powertrain is an unstable system. The principal task of the control system is to make the system stable. This is so-called power balance control in practice. The power control strategy must control the battery SOC by influencing its charge/discharge current actively, otherwise the SOC of the battery may be over upper limit or lower limit. This may cause the vehicle anchor on the road.

Several academic research groups are also working actively on this energy management technology. Yuan Zhu et al. [11] solved the power control problem of hybrid electric vehicles (HEV) by fuzzy-based and neural network-based algorithm. This method has good robustness and adaptability, but it needs much more real-time operation and its parameters setting is very difficulty. Zaimin Zhong et al. [12] proposed a battery current and SOC double close-loop feedback algorithm to solve the power balance control problem of FCHV. In this algorithm, the power demand of electric motor was fed forward as disturbance signal, and the control parameters are set and adjusted in vehicle test. Though power balance control is effective in most cycle, this method can be improved in two respects at least. Firstly, Only the power demand of electric motor was fed back, others states of system, such as current of DC/DC, battery voltage, and so on, were not used in control system. Therefore, it has potential to optimize the control strategy. Secondly, because the algorithm was based on the SOC of battery which was estimated by integral of battery current, the control system was easy to be affected by the estimated error which was

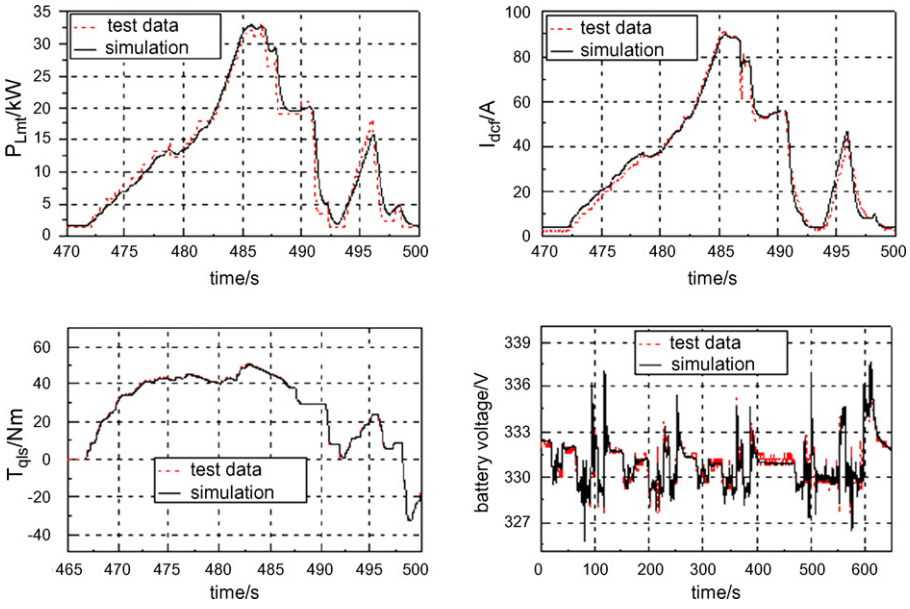

Fig. 6. Comparison between subsystem model simulation and test data.

usually caused by integral initial error and integral cumulated error.

Based on the research results of [11,12], the paper proposed a power balance control strategy which uses full-states feedback algorithm. Fig. 8 shows its framework. Where x_m: control balance position, u_{ff}: feedforward command, u_{fd}: feedback command, $\hat{x}$: states estimated by observer or estimator. These variables have relationship shown in the following equation:

$$\begin{cases} u = [\,P_{fset} \quad I_{dcfset} \quad I_{mset}\,]^T = u_{ff} + u_{fd} \\ u_{ff} = [\,P_{fset\_ff} \quad I_{dcfset\_ff} \quad I_{mset\_ff}\,]^T = [\,0 \quad 0 \quad I_{mset\_ff}\,]^T \\ u_{fd} = \begin{bmatrix} P_{fset\_fd} \\ I_{dcfset\_fd} \\ I_{mset\_fd} \end{bmatrix} = K(x\_m - \hat{x}) = K\left(\begin{bmatrix} 0 \\ 0 \\ OCV_{obj} \\ 0 \\ 0 \end{bmatrix} - \hat{x}\right) \end{cases} \tag{13}$$

where OCV_{obj}: expect position of the battery OCV, K: states feedback matrix.

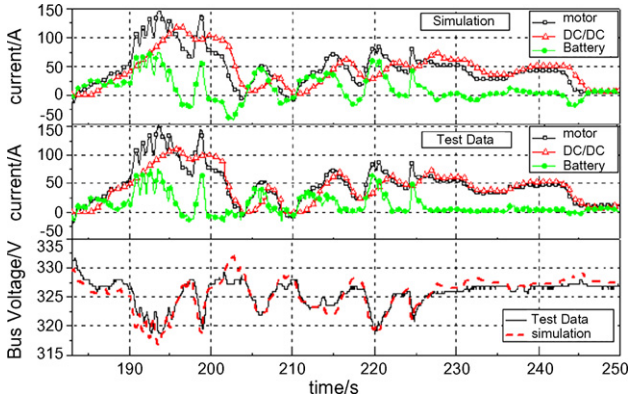

Fig. 7. Comparison example between powertrain model simulation and test data in UDDS cycle.

3.1. Feedforward generator

Feedforward generator figures out the feedforward command u_{ff} and the states balance position x_m. In practice, u_{ff} is figured out according to purpose of the driver basically and modified by some protection strategy, such as battery over discharge/charge protection strategy, FCE failure protection strategy, and so on.

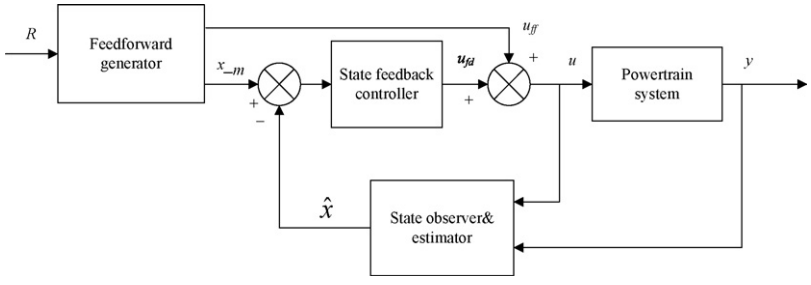

Fig. 8. Framework of the power balance control strategy.

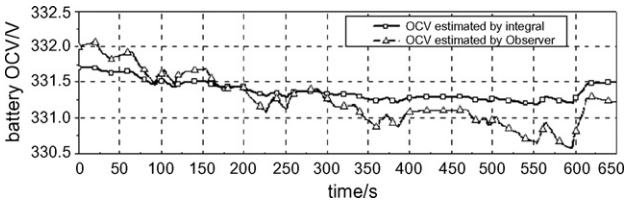

Fig. 9. Battery OCV estimated by the observer and integral.

One of the state balance positions is expected OCV of battery. Because SOC and OCV have corresponding relationship in work range of the battery [7], the battery SOC can be controlled by adjusting the state balance position.

3.2. States observer

Because battery OCV and SOC have corresponding relationship in work range, the battery SOC can be controlled by feeding back battery OCV. In the state-space model, the state U_0 denotes OCV of the battery. It can be seen that the state U_0 is very important for control system. Unfortunately the state U_0, namely battery OCV, can't be measured when powertrain is running. To solve this problem, a Luenberger state observer is designed based on the state-space model in this paper. Its state equation is showed in (14).

$$\dot{\hat{x}} = A\hat{x} + Bu + G(y - \hat{y}) = (A - GC)\hat{x} + Gy + (B - D)u \tag{14}$$

According to [10], no matter initial estimation error equals zero or not, as long as eigenvalue of matrix *A-GC* has negative real part, Eq. (15) is always right.

$$\lim_{t\to\infty}[x - \hat{x}] = 0 \tag{15}$$

Eq. (15) shows that if the feedback matrix of the observer is designed properly, the battery OCV estimated by the state observer can tend to actual battery OCV by proper speed and precision. Of course the speed and precision is inconsistent while feedback matrix of the observer is designing. Because it is independent of physical realization and the feedback matrix of the observer can be designed totally free, a most reasonable feedback matrix of the observer always can be designed finally. Fig. 9 is comparison between the battery OCV calculated by integral and that of estimated by the observer in a J1015 cycle vehicle test. According to [7], during short time range, the battery OCV calculated by integral equals to the actual value approximately.

It can be seen from Fig. 9 that the OCV estimated by observer tend to actual battery OCV by moderate speed and precision. It shows that the feedback matrix of the observer designed is reasonable.

Table 3
Signification of the state feedback

Feedback	Signification
$K_{11}(I_{dcf} - I_m)$ $K_{21}(I_{dcf} - I_m)$	Compensating delay of I_{dcf} caused by FCE slow responding feature
I_m	Making FCE power set following load power demand
$K_{13}U_0$, $K_{23}U_0$	Control SOC of the battery
$K_{14}U_1$, $K_{24}U_1$	Compensating the slow part of the battery voltage
$K_{15}U_2$, $K_{25}U_2$	Compensating the slow part of the battery voltage

3.3. States feedback controller

The key of states feedback controller is the states feedback matrix, as shown in Eq. (13). The states feedback matrix is a three rows and five columns matrix, and each element of the matrix has special signification which is shown in Table 3. Where, K_{ij} is element of the states feedback matrix.

The states feedback matrix can be designed without any constraint in control theory, but in practice, it needs to be constrained by actual conditions which are showed in Eq. (16).

$$\begin{aligned} &K_{11} - K_{12} = K_{21} - K_{22} = 1 \\ &K_{13} = K_{23} < \mathrm{a} \\ &K_{14} = K_{24},\ K_{15} = K_{25} < \mathrm{b} \\ &K_{11} < K_{21} < \mathrm{c} \\ &K_{31} = K_{32} = K_{33} = K_{34} = K_{35} = 0 \end{aligned} \tag{16}$$

where a,b,c: experimental upper limit determined by actual condition. The fifth equation of the Eq. (16) means that the electric motor torque is set according to feedforward, as shown in Eq. (13). With the constraints defined in Eq. (16), each element of the matrix is selected respectively. Proper K_{11} and K_{21} can com-

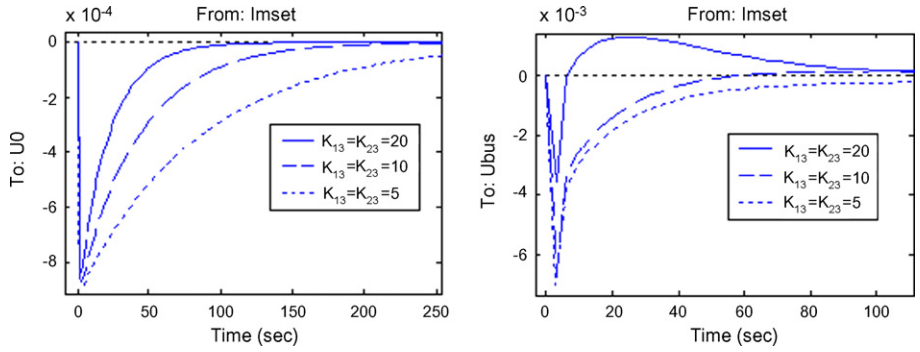

Fig. 10. Step-responding curve of the powertrain in difference K_{13} and K_{23}.

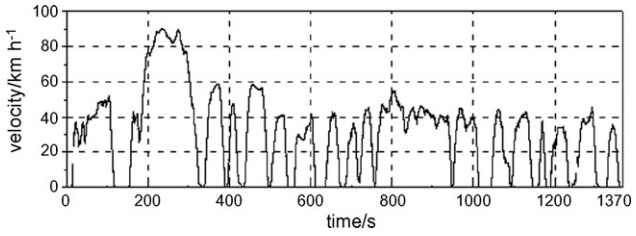

Fig. 11. Time-trace of vehicle speed (UDDS cycle).

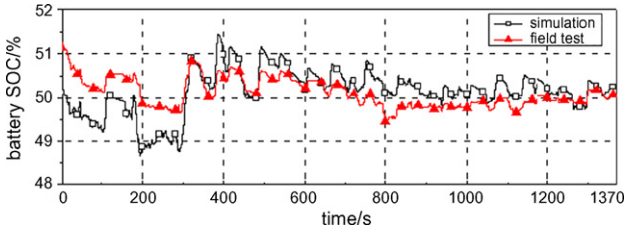

Fig. 13. Time-trace of battery SOC (UDDS cycle).

pensate delay of I_{dcf} caused by FCE slow-responding feature and cut FCE-responding time. But over large K_{11} and K_{21} may cause FCE power setting vibrating in some condition. In practice K_{11} and K_{21} are selected according to the experiment. K_{13} and K_{23} are very important for state feedback controller because they determine the stability and stable level of the control system. By analyzing the step responding of the powertrain, K_{13} and K_{23} can be selected properly. Selected system step-responding curve are presented in Fig. 10. It can be seen that the bigger K_{13} and K_{23} are, the faster converging behavior of U_0 is. But over big K_{13} and K_{23} will cause battery voltage vibrating. As shown in Fig. 10, when K_{13} and K_{23} equal 10, converging speed of U_0 is moderate and battery voltage converges to zero simplex. Like K_{13} and K_{23}, K_{14},K_{15},K_{24},K_{25} can be selected by the same way.

4. Validation the power control strategy by field test

Based on the power balance control strategy designed above, the powertrain control strategy is developed consequently and applied in START3 prototype vehicle. To validate the strategy, simulation and field test are carried out using different cycle, including J1015, UDDS, ECE-EUDC. The result of the simulation and field test shows that the powertrain control system is stable and battery SOC fluctuates between ideal upper limit and lower limit. Selected simulation and test data of UDDS cycle are presented in Figs. 11–13.

Example time-trace of the subsystems current in simulation and field test are shown in Fig. 12. It can be seen that the fuel cell provides the bulk of the power load while the battery helps with the transient part. Fig. 13 shows that battery SOC in UDDS cycle fluctuates between 48% and 52%. The object of powertrain control system is achieved excellently.

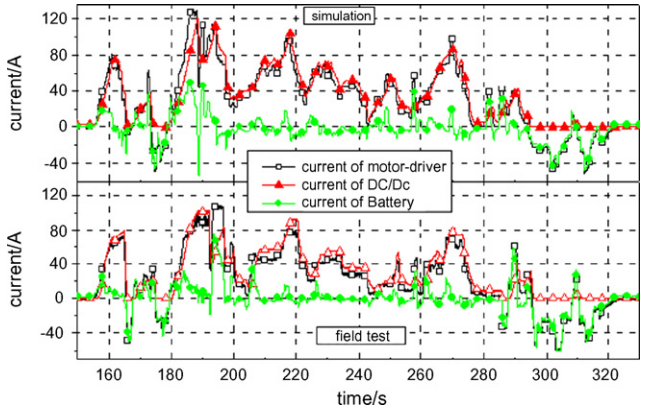

Fig. 12. Time-trace of sub-systems current (part of the UDDS cycle).

5. Conclusions

A dynamic state-space mathematic model of FCHV powertrain is developed based on the lab-testing and field vehicle testing result from START3 prototype FCHV. A vehicle simulation model is constructed by following the configuration used in START3. Model validation results confirm that the simulation model is reasonably accurate and the mathematic model is suitable for model-based control strategy development.

Based on the state-space model, a power balance control strategy is developed, which uses full-states feedback algorithm. A Luenberger state observer is designed to estimate the OCV of the battery, which makes state-feedback feasible. The state feedback controller is then designed. Results of simulation and vehicle field test show that performance of the control system is excellent.

The process described in this paper forms the model-based FCHV powertrain control system development method, which is applied in development of START3 FCHV powertrain control system successfully, and which is the general guidance for powertrain control strategy development for FCHV.

Theoretically full-states-feedback method is advanced, which enhances degree of freedom in control system design, but robustness of the control system is ordinary, and in this paper, index of control system performance is mainly discussed in frequency domain. These problems will be discussed in subsequent research project.

Acknowledgment

The authors would like to thank Shanghai Fuel Cell Vehicle Powertrain Company for their helpful support and constructive advices.

References

[1] Q Chen, B Qiu, Q Xie, et al., Fuel cell vehicle [M], Press of Tsinghua University, Beijing, 2005.
[2] T. Ishikawa, et al., Development of next generation fuel cell hybrid system—consideration of high voltage system, SAE paper, No.2004-01-1304.
[3] A. Ohkawa, Electric power control system for a fuel cell vehicle employing electric double-layer capacitor, SAE paper, No.2004-01-1006.
[4] Y. Guezennec, T.-Y. Choi, G. Paganelli, G. Rizzoni, Supervisory control of fuel cell vehicles and its link to overall system efficiency and low-level

control requirements, in: Proceedings of the American Control Conference, Denver, CO, 2003.
[5] Mohsen Mohammadian, et al., Neuro-genetic energy management for hybrid fuel cell power train, in: Proceedings of the 2006 IEEE Conference on Cybernetics and Intelligent Systems, Singapore, 13 December 2006.
[6] T. Markel, et al., Journal of Power Sources 110 (2002) 255–266.
[7] Wei Xuezhe, Study on Li-ion power battery management system in fuel cell vehicle, Dissertation. Tongji University, submitted for publication.
[8] M. Hou, P. Ming, D. Sun, et al., Fuel Cells 4 (1–2) (2004) 101–104.
[9] Chengqian Zhang, System Identification and Parameters Estimation, China Machine Press, Beijing, 2001.
[10] R.C. Dirf, Modern control system, Science Press, Beijing, 2002.
[11] Zhu Yuan, The Four-steps Design Method of Energy Management for Hybrid Electric Vehicle. Dissertation. Tshinghua University submitted for publication.
[12] Zhong Zaimin, Wei Xuezhe, Sun Zechang, Journal of Tongji University (Natural Science) 6 (2004) 758–761.